Supporting Information

A Direct N-butane Solid Oxide Fuel Cell Using $Ba(Zr_{0.1}Ce_{0.7}Y_{0.1}Yb_{0.1})_{0.9}Ni_{0.05}Ru_{0.05}O_{3-\delta}$ Perovskite as the Reforming Layer

Dongfeng Wang[1], Shao Ing Wong[2], Jaka Sunarso[2], Meigui Xu[1], Wei Wang[1], Ran Ran[1], Wei Zhou[1,*], Zongping Shao[1,3,*]

[1]Jiangsu National Synergetic Innovation Center for Advanced Materials (SICAM), State Key Laboratory of Materials-Oriented Chemical Engineering, College of Chemical Engineering, Nanjing Tech University, Nanjing 210009, P. R. China

[2]Research Centre for Sustainable Technologies, Faculty of Engineering, Computing and Science, Swinburne University of Technology, Jalan Simpang Tiga 93350, Kuching, Sarawak, Malaysia

[3]WA School of Mines: Minerals, Energy and Chemical Engineering, Curtin University, Perth, Western Australia 6845, Australia

Corresponding Authors

Wei Zhou - Email: zhouwei1982@njtech.edu.cn

Zongping Shao - Email: shaozp@njtech.edu.cn

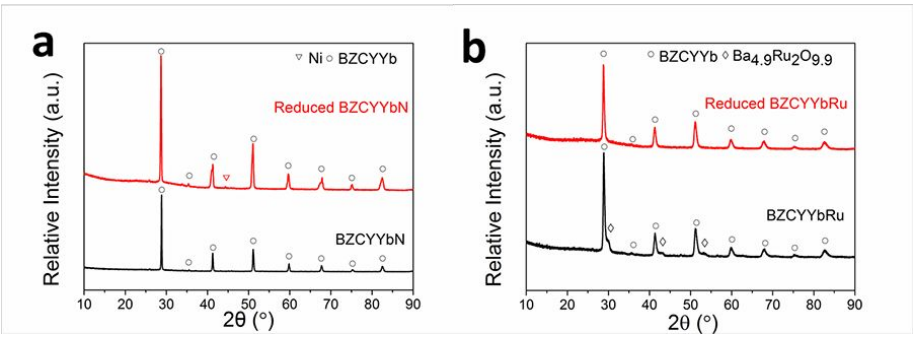

Figure S1. Powder XRD patterns of **(a)** BZCYYbN **(b)** BZCYYbRu samples together with their reduced samples. The catalyst powders were reduced by 80 mL min^{-1} H_2 for 2 h at 800 °C.

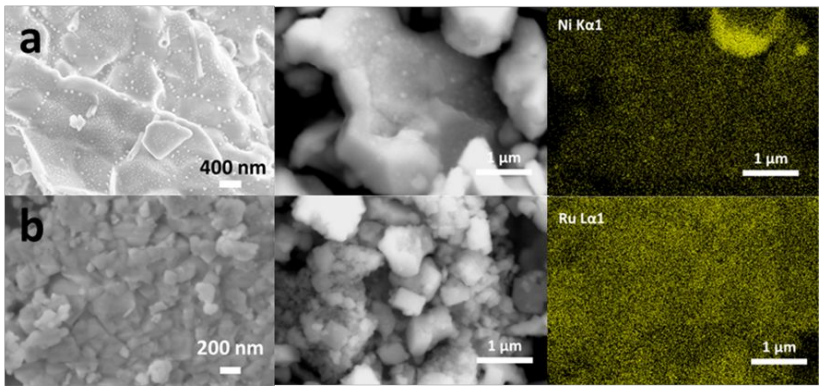

Fig. S2. Surface microstructure of **(a)** BZCYYbN and **(b)** BZCYYbRu characterized by scanning electron microscope-energy dispersive X-ray dispersive spectroscopy (SEM-EDX). The catalyst powders were reduced by 80 mL min^{-1} H_2 for 2 h at 800 °C.

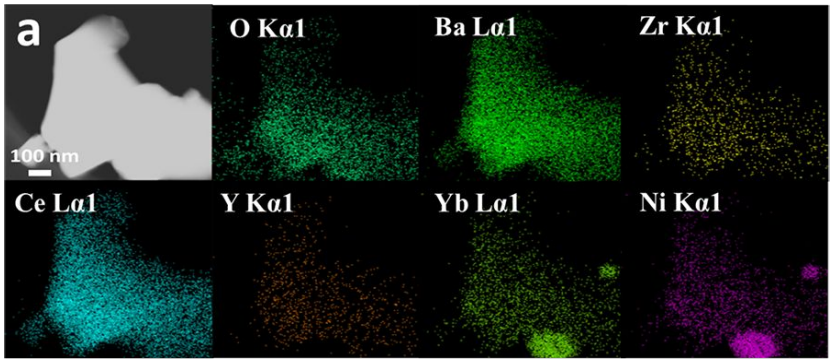

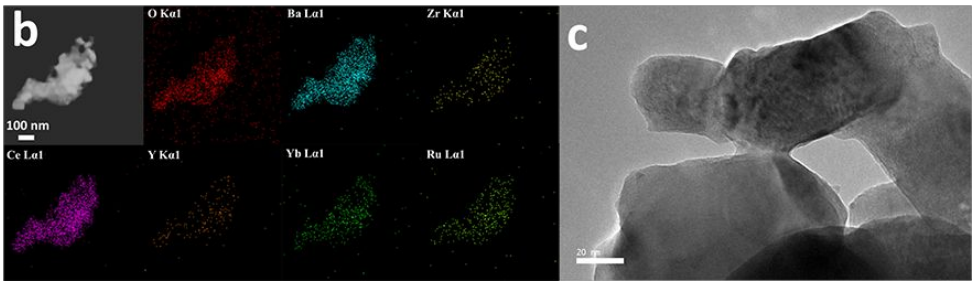

Figure S3. The metal dispersion and precipitation of **(a)** BZCYYbN and **(b)** BZCYYbRu characterized by transmission electron microscope-energy dispersive X-ray spectroscopy (TEM-EDX). The catalyst powders were reduced by 80 mL min^{-1} H_2 for 2 h at 800 °C. (The energy intensity of Ni Kα1 is similar to that of Yb Lα1, with overlapping spectra.). **(c)** High-resolution transmission electron microscopy (HR-TEM) of BZCYYbRu.

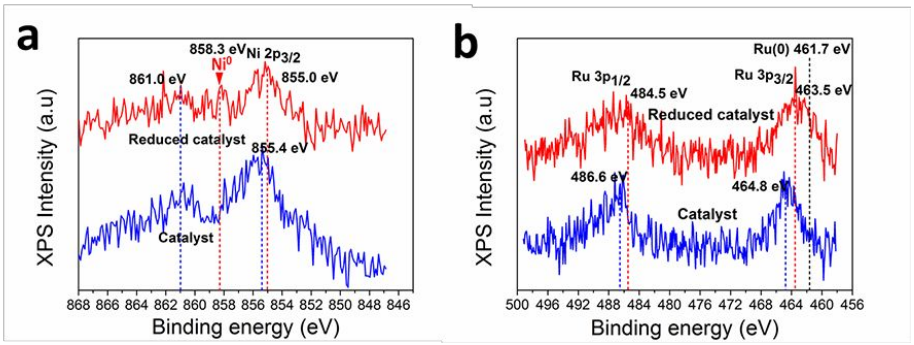

Figure S4. The metal oxidation state of **(a)** BZCYYbN and **(b)** BZCYYbRu were characterized by Ni 2p and Ru 3p X-ray photoelectron spectroscopy (XPS). The catalyst powders were reduced by 80 mL min^{-1} H_2 for 2 h at 800 °C.

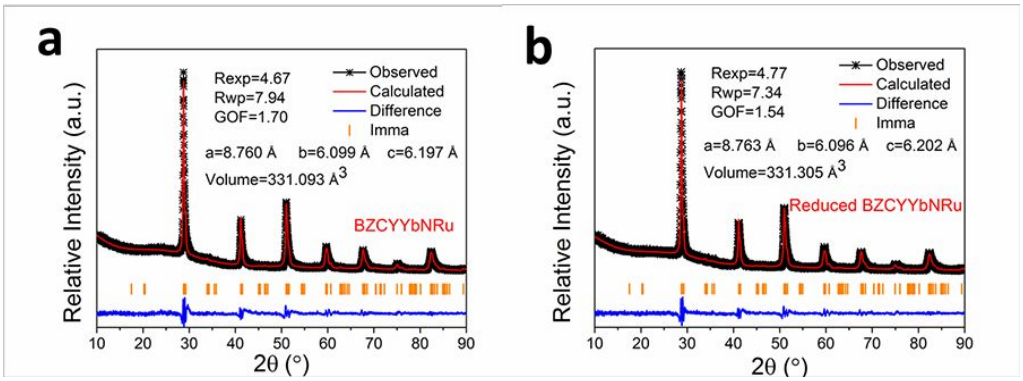

Figure S5. Refined XRD profiles of **(a)** BZCYYbNRu and **(b)** reduced BZCYYbNRu sample.

Table S1. BET surface area of BZCYYbN, BZCYYbRu, and BZCYYbNRu. The reduced catalysts were treated with 80 mL min^{-1} H_2 at 800 °C for 2 h.

Table S1. Characterization of catalyst specific surface area

Sample	BZCYYbN	BZCYYbNRu	BZCYYbRu
Reduced catalyst	1.328	3.378	2.538
Catalyst	0.976	4.465	3.191

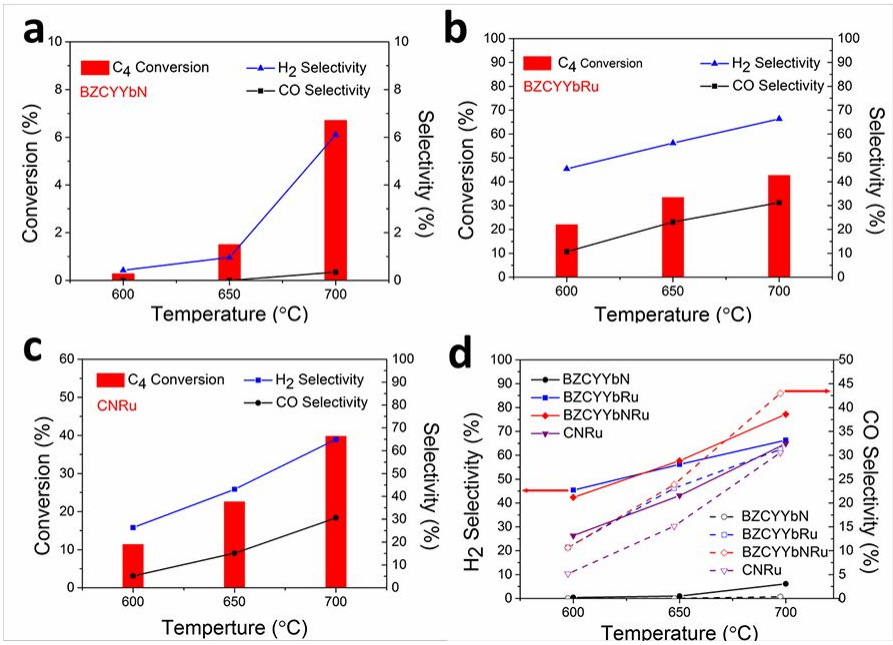

Figure S6. Steam reforming conversion rate and CO and H_2 selectivity of **(a)** BZCYYbN, **(b)** BZCYYbRu, **(c)** CNRu catalyst. **(d)** The selectivity comparison between various catalysts with the fuel of n-butane (with the ratio of H_2O:C = 0.5) during 600 °C to 700 °C. The steam reforming catalyst was reduced by H_2 for 2 h at 800 °C before the test.

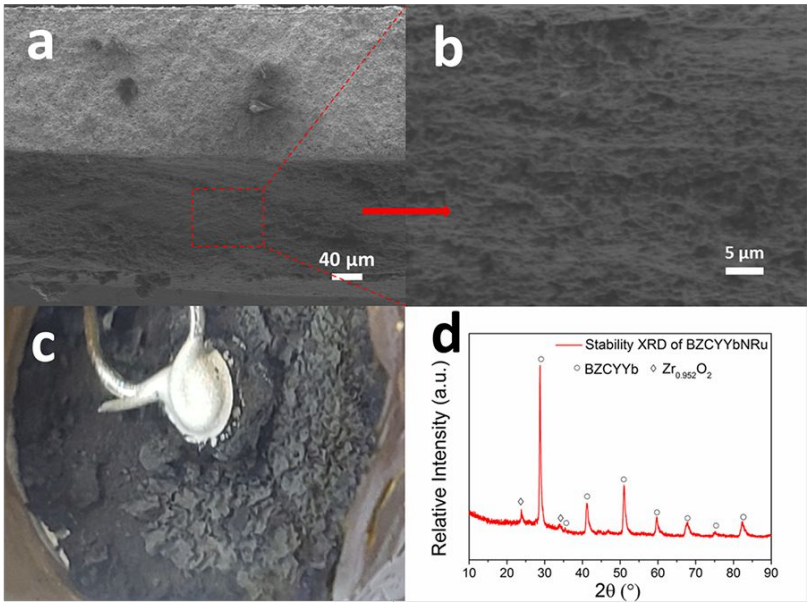

Figure S7. SEM image that shows **(a)** the overall surface structure of the BZCYYbNRu catalyst-attached anode after stability test, and **(b)** the magnified parts of the catalyst surface. **(c)** The digital image of the anode without catalyst layer after the stability test. **(d)** XRD pattern of the BZCYYbNRu after the cell stability test. ($Zr_{0.952}O_2$, PDF 01-081-1329)

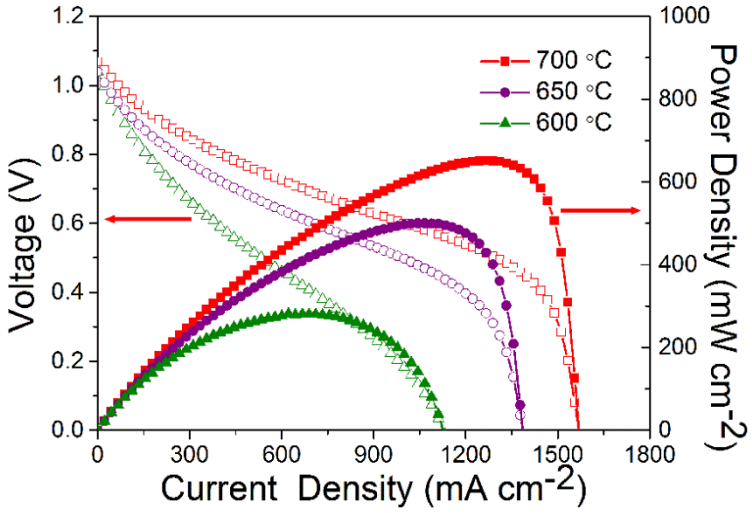

Figure S8. I–V and I–P of fuel cell performance with the BZCYYbNRu anode steam reforming catalyst when operated at 600-700 °C using n-butane (with the ratio of H_2O:C = 1, and the flow rate of C_4H_{10} was 5 mL min^{-1}, the flow rate of H_2O was 20 mL min^{-1}) as the fuel. The single fuel cell was reduced by H_2 for 2 h at 800 °C before test.

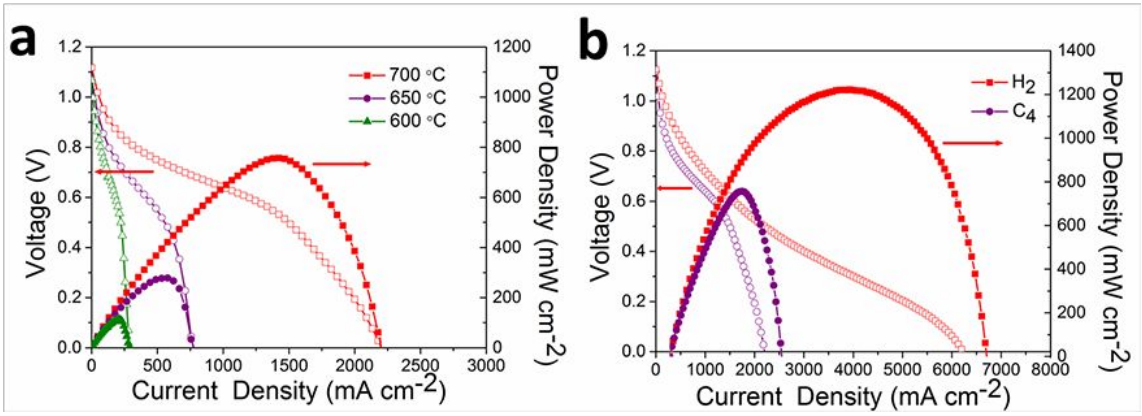

Figure S9. I–V and I–P of fuel cell performance with the BZCYYbN anode steam reforming catalyst when operated at 600-700 °C using n-butane fuel (with the rate of H_2O:C = 0.5) **(a)** and at 700 °C using H_2 fuel **(b)** for comparison. The single fuel cell was reduced by H_2 for 2 h at 800 °C before test.

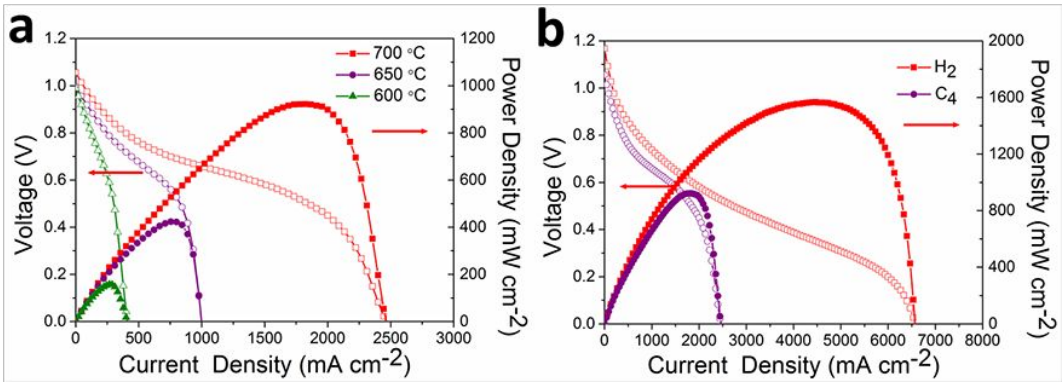

Figure S10. I–V and I–P of fuel cell performance with the BZCYYbRu anode steam reforming catalyst when operated at 600-700 °C using n-butane fuel (with the rate of H_2O:C = 0.5) **(a)** and at 700 °C using H_2 fuel **(b)** for comparison. The single fuel cell was reduced by H_2 for 2 h at 800 °C before test.

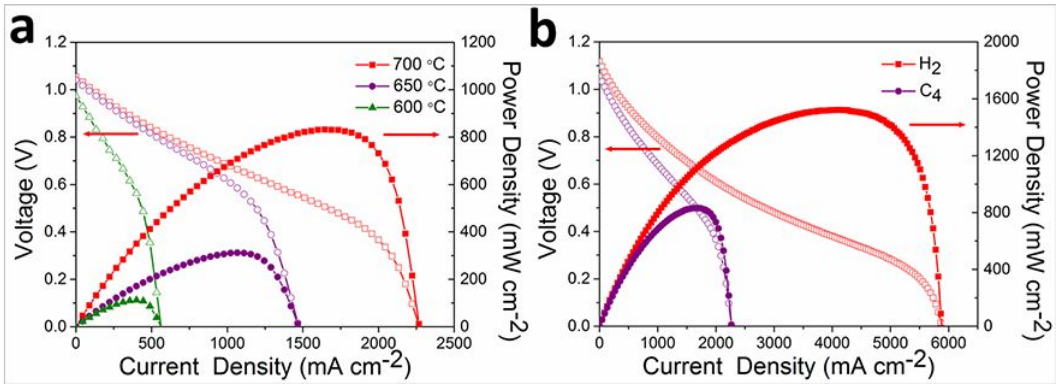

Figure S11. I–V and I–P of fuel cell performance without anode steam reforming catalyst when operated at 600-700 °C using n-butane fuel (with the rate of H_2O:C = 0.5) **(a)** and at 700 °C using H_2 fuel **(b)** for comparison. The single fuel cell was reduced by H_2 for 2 h at 800 °C before test.

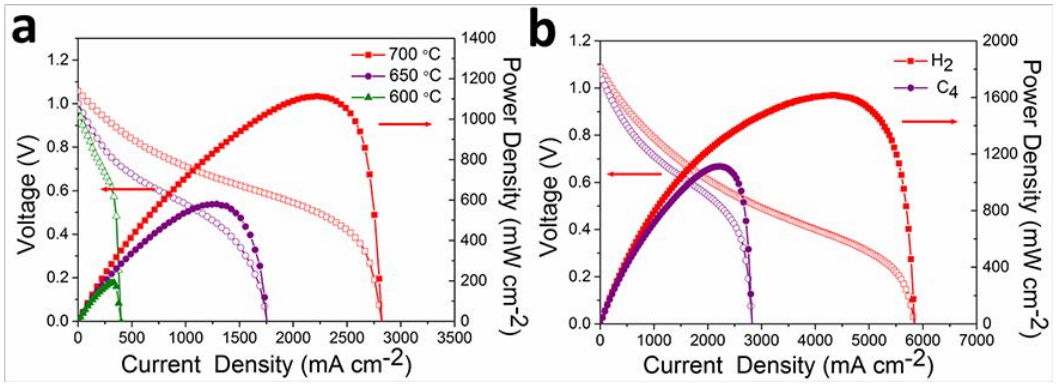

Figure S12. I–V and I–P of fuel cell performance with the BZCYYbNRu anode steam reforming catalyst

when operated at 600-700 °C using n-butane fuel (with the rate of H_2O:C = 0.5) **(a)** and at 700 °C using H_2 fuel **(b)** for comparison. The single fuel cell was reduced by H_2 for 2 h at 800 °C before test.

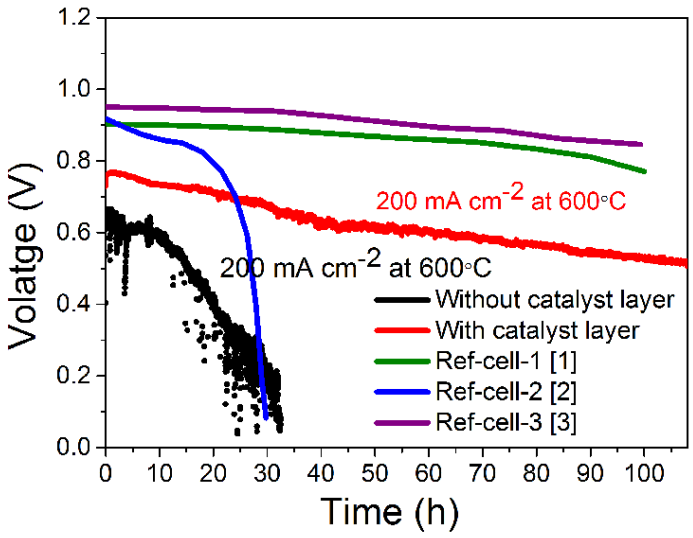

Figure S13. Comparison of the stability performance of various SOFCs operated with hydrocarbon fuels in direct internal steam reforming operations. Stability test for fuel cell with the BZCYYbNRu anode steam reforming catalyst when operated at 600 °C with n-butane (with the rate of H_2O:C = 0.5), and such a single fuel cell was reduced by H_2 for 2 h at 800 °C before test. Ref-cell-1-3 are the performance of the single cell in the cited literature, corresponding to [1]-[3] in the supporting references respectively.

Table S2. Comparison of the stability performance of our SOFCs and those from literature when operated with hydrocarbon fuels in direct internal steam reforming operations.

Table S2. Comparison of the stability performance of SOFC on hydrocarbon fuels in direct internal steam reforming operations					
Anode material	**Operating temperature (°C)**	**Gas composition (Steam/Carbon)**	**Degradation rate @ j mAcm^{-2}**	**Remarks**	**Ref.**
BZCYYNRu -Ni-YSZ	**600**	**C_4H_{10}(10ml)-Ar(50ml) S/C = 0.5**	**2.32×10^{-3} V h^{-1} in 108 hours @ j = 200 mA cm^{-2}**	**LT operation**	**This paper**
Ni-YSZ	**600**	**C_4H_{10}(10ml)-Ar(50ml) S/C = 0.5**	**1.86×10^{-2} V h^{-1} in 32 hours @ j = 200 mA cm^{-2}**	**LT operation**	**This paper**
PdO-Ni-YSZ	**600**	**C_4H_{10}(10ml)-H_2(10ml)-N_2(60ml) S/C = 3**	**1.34×10^{-3} V h^{-1} in 100 hours @ j = 150 mA cm^{-2}**	**LT operation**	**[1]**
PdO-Ni-YSZ	**600**	**C_4H_{10}(10ml)-N_2(90ml) 3% H_2O**	**2.82×10^{-2} V h^{-1} in 30 hours @ j = 150 mA cm^{-2}**	**LT operation**	**[2]**
PdO-Ni-YSZ	**600**	**C_4H_{10}(10ml)-H_2(10ml)-N_2(60ml) S/C = 3**	**1.08×10^{-3} V h^{-1} in 100 hours @ j = 100 mA cm^{-2}**	**LT operation**	**[3]**

References

[1] Thieu, C. A.; Park, S.; Kim, H.; Ji, H. I.; Lee, J. H.; Yoon, K.J.; Yang, S.; Son, J. W. Improved Electrochemical Performance and Durability of Butane-operating Low-temperature Solid Oxide Fuel Cell Through Palladium Infiltration. *Inter. J. Energy Res.* **2020**, 44:9995-10007.

[2] Thieu, C. A.; Ji, H. I.; Kim, H.; Yoon, K. J.; Lee, J. H.; Son, J. W. Palladium Incorporation at the Anode of Thin-film Solid Oxide Fuel Cells and its Effect on Direct Utilization of Butane Fuel at 600 °C. *Appl. Energy* **2019**; 243:155-164.

[3] Thieu, C. A.; Yang, S.; Ji, H. I.; Kim, H.; Yoon, K. J.; Lee, J. H.; Son, J. W. Effect of Secondary Metal Catalysts on Butane Internal Steam Reforming Operation of Thin-film Solid Oxide Fuel Cells at 500-600 °C. *Appl. Catal. B: Environ.* **2020**, 263:118349.